Proceedings of the ASME 2017 Fluids Engineering Division Summer Meeting
FEDSM2017
July 30-August 3, 2017, Waikoloa, Hawaii, USA

FEDSM2017-69171

THE AERODYNAMIC CHARACTERISTICS OF THE PANTOGRAPH WHEN THE TRAIN PASSES THROUGH THE TUNNEL

Dilong Guo
Institute of mechanics, Chinese academy of sciences
Beijing, China

Wen Liu
Institute of mechanics, Chinese academy of sciences
Beijing, China

Junhao Song
Institute of mechanics, Chinese academy of sciences
Beijing, China

Ye Zhang
Institute of mechanics, Chinese academy of sciences
Beijing, China

Guowei Yang
Institute of mechanics, Chinese academy of sciences
Beijing, China

ABSTRACT

The aerodynamic force acting on the pantograph by the airflow is obviously unsteady and has a certain vibration frequency and amplitude, while the high-speed train passes through the tunnel. In addition to the unsteady behavior in the open-air operation, the compressive and expansion waves in the tunnel will be generated due to the influence of the blocking ratio. The propagation of the compression and expansion waves in the tunnel will affect the pantograph pressure distribution and cause the pantograph stress state to change significantly, which affects the current characteristics of the pantograph. In this paper, the aerodynamic force of the pantograph is studied with the method of the IDDES combined with overset grid technique when high speed train passes through the tunnel. The results show that the aerodynamic force of the pantograph is subjected to violent oscillations when the pantograph passes through the tunnel, especially at the entrance of the tunnel, the exit of the tunnel and the expansion wave passing through the pantograph. The changes of the pantograph aerodynamic force can reach a maximum amplitude of 106%. When high-speed trains pass through tunnels at different speeds, the aerodynamic coefficients of the pantographs are roughly the same.

1. INTRODUCTION

Pantograph is one of the core components of high-speed electrified train, The electric energy needed for continuous operation of high-speed train is usually obtained from the catenary by using the pantograph installed on the roof. In order to ensure that the electric energy can be obtained continuously from the catenary during the running of the train. The contact force between the slide of the pantograph and the catenary should be maintained under the condition of relative sliding. If the contact force is insufficient, it will lead to the increase of the contact resistance, the pantograph and catenary may be separated, the electric arc generates, and thus the quality of current is affected, and catenary network is damaged [1,2]. The stable contact state needs to be maintained by a suitable contact force between the slide plate and the catenary. With the increase of HST speed, the complex-shaped pantograph will be disturbed by the airflow and starts to oscillate.

In addition to the speed effect, high-speed trains usually need to pass bridges, tunnels and other constructions. The changes of scenes cause significant changes in the flow field around the train, the forces of the components of the train will change. For example, when a high-speed train passes through a tunnel, the air flow is restricted by the effect of the tunnel wall as the space becomes smaller instantaneously. The compression waves are generated when the train nose enters the tunnel, called the initial compression wave, the initial compression waves propagate to the tunnel exit at the local sound speed, and reflect to the tunnel entrance in the opposite direction in the form of expansion waves. In addition, a small part of the compression waves radiate to the surrounding environment in the form of micro-pressure wave. The propagation of the pressure wave in the tunnel causes the air pressure change, which causes complicated pressure changes in the tunnel and the body of the train. The violent change of the pressure wave may cause the fluctuation of the lift and drag force of the

pantograph, which makes the contact force of the slide and the catenary fluctuate violently, and affects the current collection [3-6].

The aerodynamics of the pantograph of high speed train is mainly studied by experimental and numerical methods in the literatures. M.Bocciolone studied the effect of the shape of the slide on the pantograph aerodynamics using the method of wind tunnel experiments -and mainly considered the turbulence effect [7]. By using the numerical method, Li studied the lift characteristics of the pantograph under the condition of pores and closed pores [8]. The unsteady aerodynamic force characteristics of the pantograph were studied by Guo and Yao [9, 10]. However, for the aerodynamic force of the pantograph when high-speed trains pass through the tunnel, the relevant studies have not been found. Therefore, it is necessary to simulate the dynamic process of high speed train passing through the tunnel, so as to provide the fundamentals for the pantograph design.

2. THE COMPUTATIONAL MODEL AND DOMAIN

Due to the complicated flow field around the pantograph, it is difficult to solve the engineering problems of the pantograph by using the theoretical analysis method. There are mainly two methods to research the aerodynamic problems of the pantograph, including experimental method and numerical calculation method. The experimental research methods include the real train test and the model test, however, the two experimental methods have their own shortcomings respectively. For example, the appropriate balances are not obtained in real train test and moving model test, and the relative motion between the train and tunnel cannot be satisfied in wind tunnel test. The numerical simulation method can be relatively fast and effective to simulate the performance, so it is now widely used.

The preliminary numerical calculation work includes the establishment of computational model, the division of the calculation grid and settings of the boundary conditions. Each of these parts is directly related to the accuracy of the results. The geometric model, the meshes and the boundary conditions settings are given below.

The pantograph is located at the roof of the high-speed train, the impact of train body to the pantograph flow field must be considered. In addition, the blockage ratio has a great influence on the strength of the compression wave and the expansion wave, so the train body is added into the geometric model. The train model is composed of three groups including head, intermediate, and tail carriage. Since the windshield and the bogies of the train have little influence on the flow field of the pantograph, the simplified treatment is carried out. The geometric model of the pantograph is basically the same as that of the actual pantograph, and the position of the pantograph is located at the front end of the intermediate carriage. The area of the tunnel section is 70m^2, which is shown in Fig.1, the train model and pantograph model are shown in Fig.2 and Fig.3.

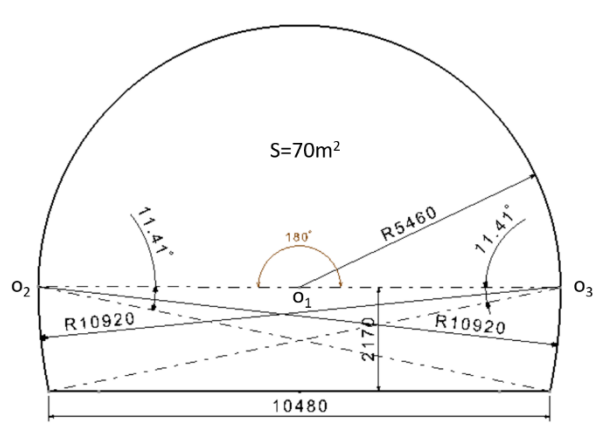

Fig.1 The schematic diagram of the tunnel (unit: mm).


Fig.2 The schematic diagram of the train


Fig.3 The schematic diagram of the pantograph

The pressure wave generated by the train running in different tunnel length varies greatly. When the tunnel section, train speed and train length are given, there is the most unfavorable tunnel length. In this paper, the tunnel length is based on the EN-14067 [11] and is given in Equation (1).

$$L_{tu,crit} \approx \frac{L_{tr}}{4}\frac{c}{v_{tr}}\left(1+\frac{c}{v_{tr}}\right) \quad (1)$$

Where L_{tr} is the train length, c is the speed of sound, and v_{tr} is the train running speed. In this study, the train length is 78m, the speed of sound is 340m/s, the train speed is 97.22m/s. the most unfavorable tunnel length is 306.7m, for convenience, taking the tunnel length of 310m. The relative position between the train and tunnel at the initial moment is shown in Fig.4. The computational domain is shown in Fig.5.

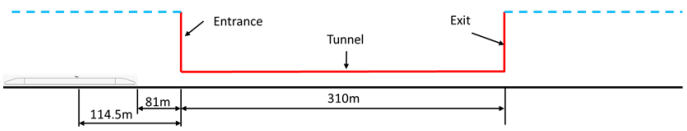

Fig.4 The schematic diagram of between the train and tunnel

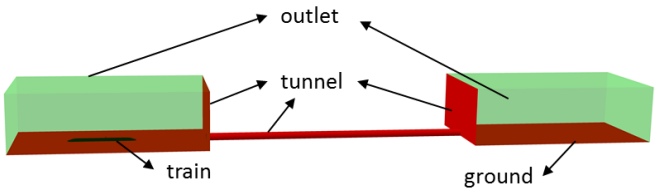

Fig.5 The schematic diagram of the computational domain

3. COMPUTATIONAL ALGORITHMS AND BOUNDARY CONDITIONS

The commercial CFD code STAR-CCM+ is used to simulate the process of train passing through the tunnel [12]. The software is wildly used in the automotive industry. The STAR-CCM+ integrates the pre-processing, solver, post-processing into a package, and it can generate high quality mesh for complex geometry. The STAR-CCM+ provides several meshing strategies that are suitable for different applications, in this study, the trimmed cell mesher is selected to generate volume mesh.

The air flow caused by the process of high-speed train passing through the tunnel is very complicated, which involves both the unsteady flow characteristics and the propagation of the pressure wave caused by the train passing through the tunnel. In this study, to simulate the details in the flow fields accurately, the improved delayed detached eddy simulation (IDDES) formulation is selected; this method combines DDES with an improved RANS-LES hybrid model aimed at wall modeling in LES when the grid resolution supports it. To save the mesh resolution near the wall, the wall functions is used. Considering the train's running speed, the coupled implicit unsteady solver is selected. The inviscid flux term is discretized using the Weiss-Smith preconditioned Roe's flux-difference splitting scheme. The transient term is discretized -using an Euler implicit two-order temporal scheme. Since solving for unsteady flows requires a dual time-stepping, with inner iterations in pseudo-time, the physical time-step is 0.002s, the inner iteration steps are 15.

To simulate the relative motion between the train and the tunnel, the overset grid technique is used, the overset grid techniques offer flexibility in handling the problems that involve multiple bodies in relative motion, in the method, the computational domain is covered by a number of grids which overlap with each other in an arbitrary manner. When the component grids move relative to each other, only the location of boundary points at overlapping interfaces that are involved in interpolation changes, the grid points do not need to be regenerated and the grids retain their topology and geometrical properties. In this study, the overset meshes include one background region and one overset region, the overset region contains the train model and pantograph model. The meshes is shown in Fig.6.

Fig.6 The meshes of the computational model

The volume meshes of the background region are about 8.7 millions, the volume meshes of the overset region are about 8.2 millions. To resolve the detail flow adjacent the pantograph, a density zones is specified to refine the volume meshes. In the mesh density zones, the mesh size is 30mm. To resolve the boundary layer around the train and the pantograph, a prism layer of 10 cells has been created in a belt of thickness 0.02m around the train. the stretch ratio is 1.2, the first layer is about 8 $\times 10^{-4}$m, which ensures that Y plus ranges from 30 to 100. In the background mesh, the mesh size that involved to be overlapped is 0.25m according to the temporal discretization scheme and the velocity of the train and the time step. The mesh size around the overset meshes is 0.25m too, which enforces the overlapping zone contain at least 4-5 cell layers in both background and overset meshes.

The whole calculations are carried out in the computer cluster at Supercomputing Centre of Chinese Academy of Sciences.

The boundary conditions include pressure outlet, no-slip wall. In the outlet which is shown in the Fig.5, the pressure outlet boundary condition is employed. The ground and the tunnel and the train is set as no-slip boundary condition.

4. ALGORITHM VALIDATION

To validate the computational method and mesh resolution, the wind tunnel test data and the CRH380A 1: 8 scaled model are compared. The wind tunnel test model is shown in Fig. 7 (a). Fig. 7 (b) shows the distribution of spatial grids for CFD computation. In the wind tunnel test, the velocity of inflow is 60m/s, the Reynolds based on the characteristic length of train model height is about 1.8×10^{6}. The mesh independence test and wind tunnel test data results comparison are shown in the Table 1, in the mesh independence test, the mesh size in the density zone is 10mm, 30mm, 60mm, respectively, as shown Table 1, when the mesh size is 10mm, 30mm, respectively, there are little influence on the total predicated drag coefficients, and the predicted results are in good agreement with the experimental results. Therefore, the mesh size in the density zone of pantograph mesh is set 30mm.

Table.1 Mesh independence test and experimental comparison

Mesh size (mm)	Total drag coefficient	Error
10	0.3261	1.7%
30	0.3136	2.18%
120	0.3072	4.2%

EXP	0.3206

(a) Wind tunnel test model

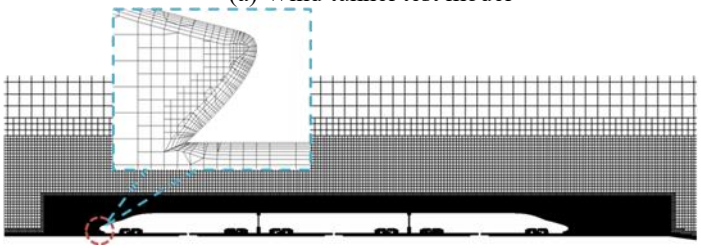

(b) The distribution of the spatial grid

Fig. 7 Wind tunnel test model and space distribution grid

5. RESULTS AND DISCUSSION

Since the tunnel length is designed according to the speed of 350km/h, we take the speed of 350km/h as an example to analyze the characteristics of the flow field around the pantograph and aerodynamic force characteristics when train passes through the tunnel. For comparison, the state of the high-speed train passing through the tunnel at the speed of 300km/h was calculated too.

5.1 THE FLOW STRUCTURE OF THE WAKE FIELD OF THE PANTOGRAPH

When the train is located at the different position of the tunnel, the positions of the compression waves and the expansion waves in the tunnel are different, which causes the pressure difference in different positions. In the Fig.8, the pressure contours of the tunnel wall are shown, it can be seen that the pressure of the tunnel wall varies greatly when the train is located at the different position of the tunnel, which affects the flow structure of the wake field of pantograph.

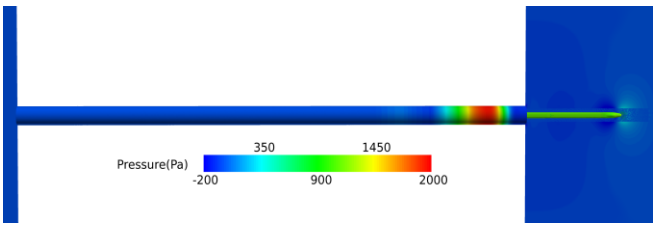

(a) At the entrance

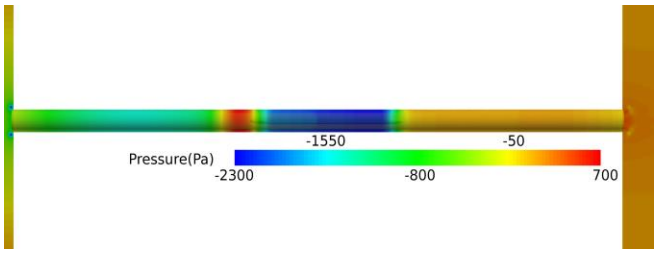

(b) In the middle

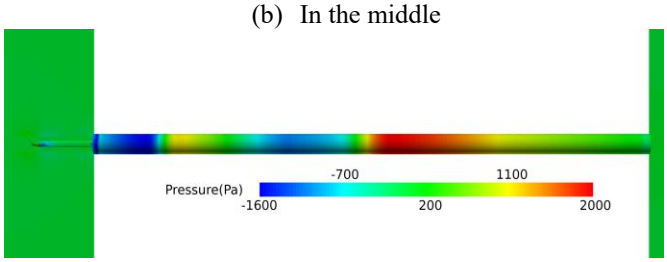

(c) At the exit

Fig. 8 The pressure contours of the tunnel wall

The flow structure of the wake field of pantograph is very complicated. In the course of high-speed train passing through the tunnel, the flow field around the pantograph is obviously different due to the different relative position between the train and the tunnel. Here, the difference is represented by iso-surface contours of Q and the pressure contours on plane of the symmetry near the pantograph region. Q iso-surface contours can describe the position of the vortices. In the Fig.9, the Q is equal to 600. The position of Fig.9 (a) is at the entrance of the tunnel, the position of Fig.7 (b) is in the middle of the tunnel, the position of Fig.9(c) is at the exit of the tunnel. It can be seen from the three contours that a series of vortices form near the pantograph region and flow to the rear of the train when the train is running at high speed. When the train is located at the entrance, the middle and the exit of the tunnel, the wake of the pantograph is full of strong vortices, but there are obvious difference of the vortices at different position. At the exit and in the middle of the tunnel, the scope of the vortices is larger than that at the entrance, especially at the exit of the tunnel, there are strong vortices generated on the tunnel wall because of the great different pressure inside and outside the exit of the tunnel, which causes strong aerodynamic force fluctuations when the train left the tunnel.

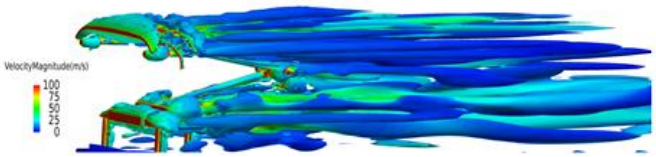

(a) At the entrance

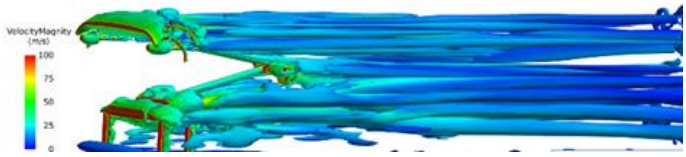

(b) In the middle

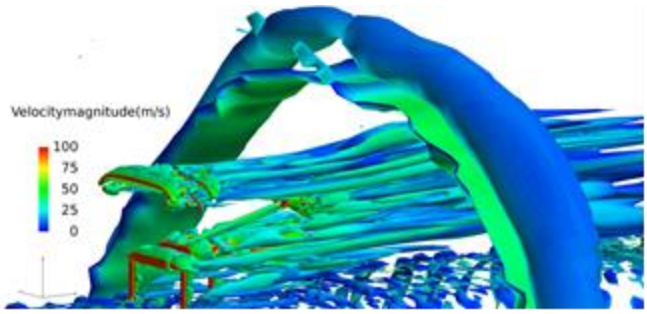

(c) At the exit

Fig.9 The Q iso-surface contours at the different position of the pantograph

The pressure contours at the symmetry plane near the pantograph region when the pantograph is located at different positions of the tunnel are shown in Fig.10. When the pantograph is at the entrance of tunnel, the pressure near the pantograph region changes little due to the proximity of the infinite space at the entrance. When the pantograph is located in the middle of the tunnel, the pressure in the vicinity of the pantograph varies greatly due to the limitation of annular space between the tunnel and train, meanwhile, the compression wave and the expansion wave intensify the pressure changes. At the exit of the tunnel, the high pressure scope of the pantograph slide is larger than in the middle of the tunnel, and the pressure change in the region near the pantograph is larger than that at the entrance of the tunnel.

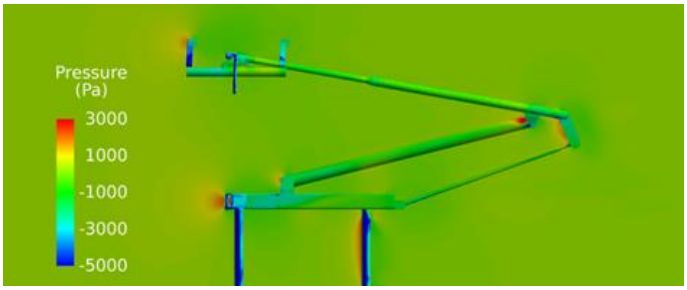

(a) At the entrance

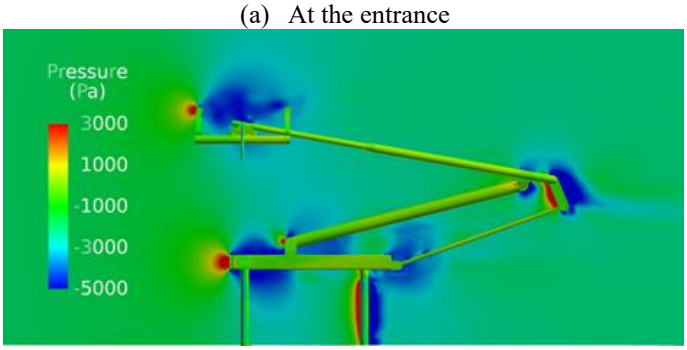

(b) In the middle

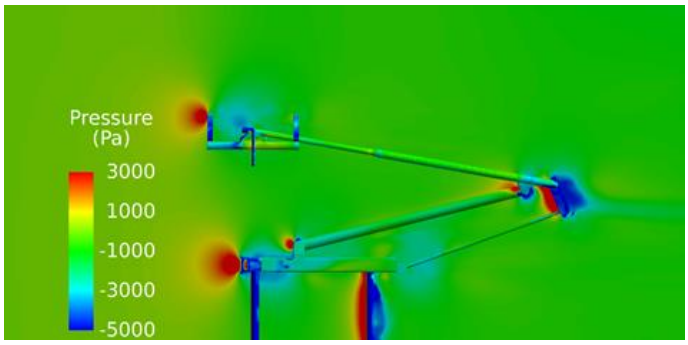

(c) At the exit

Fig.10 The pressure contours at the different position of the pantograph

5.2 THE VARIATION OF THE ARRODYNAMIC FORCE OF THE PANTOGRAPH ALONG THE TUNNEL

When the train is entering the tunnel, the compression wave is generated ahead of the train due to limitation of the tunnel wall to the airflow. The compression wave propagates to the exit at the speed of sound, at the exit of the tunnel, the part of the wave is radiated out of the tunnel in the form of micro-pressure wave, and the other part is reflected to the tunnel in the form of expansion wave. In addition because the space around the train is significantly reduced, the pressure around the pantograph increases. In the Fig.11, the aerodynamic drag variation of the pantograph when the train is passing through the tunnel at the speed of 350km/h is shown. It can be seen that the aerodynamic drag of the pantograph increases greatly when the train passing through the tunnel, meanwhile, the aerodynamic drag varies greatly. When the train is far away from the entrance of the tunnel, the aerodynamic drag of the pantograph is about 1940N, at the time of t=1s, the train head has entered the tunnel about 20 meters, at this moment, the pantograph is about 14.5 meters away from the tunnel entrance. The aerodynamic drag of the pantograph increases dramatically, at the time of t=1.23s, after entering the tunnel 5 meters, the aerodynamic drag of the pantograph reaches a high value of 2400N. After a period of stability, the aerodynamic drag increases further, at the time of t=2.87s, it reaches the value of 2810N, then decreases dramatically, this is because the expansion wave reflected from the tunnel exit passes through the pantograph, which reduces the surface pressure of the pantograph and then reduces the aerodynamic drag. After that, the surface pressure on the pantograph gradually restores and the aerodynamic drag of the pantograph increases. At the time of t=4.36s, the pantograph begins to leave the tunnel exit, the pressure inside and outside the tunnel varies greatly because of the expansion wave radiating to the exit, the aerodynamic drag of the pantograph varies very intensely. At 0.116s, the aerodynamic drag of the pantograph reduces from 3400N to 1650N. The change rate reaches up to 106%. In the Fig.10, the aerodynamic lift variation of the pantograph when the train is passing through the tunnel is shown. It can be seen that the aerodynamic lift of the pantograph is consistent with the trend

of the aerodynamic drag. As the aerodynamic lift is small, the oscillation of the aerodynamic lift is large, which exhibits obvious unsteady characteristics.

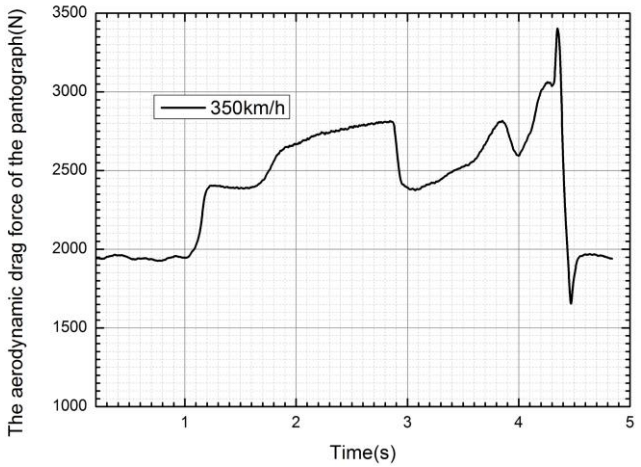

Fig.11 The aerodynamic drag variation of the pantograph .vs. time

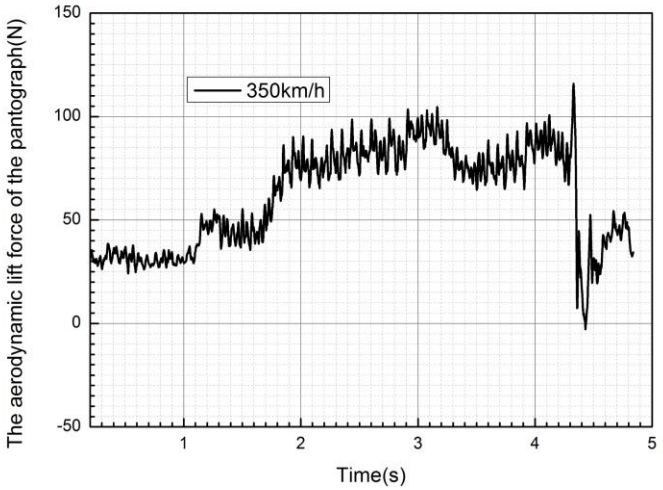

Fig.12 The aerodynamic lift variation of the pantograph .vs. time

5.3 THE VARIATION OF THE ARRODYNAMIC FORCE OF THE PANTOGRAPH WITH DIFFERENT SPEED

When the train passes through the tunnel at different speeds, the position where the compression and expansion wave act on the train is different due to the different train speed. In order to analyze the relationship between the aerodynamic force of the pantograph and its position in the tunnel, the time coordinate is converted to the space, the leading point of the pantograph is taken as origin, then the aerodynamic forces are non-dimensionlized by the running speed of the train.

In order to facilitate the comparison, the coefficients of aerodynamic forces are defined as follows:

The coefficient of aerodynamic drag C_d ,

$$C_d = \frac{2F_x}{\rho v^2 S} \tag{2}$$

The coefficient of aerodynamic lift C_l ,

$$C_l = \frac{2F_y}{\rho v^2 S} \tag{3}$$

In the Equation (2) and (3), F_x is the aerodynamic drag force, F_y is the aerodynamic lift force, ρ is the density of the air, v is the running speed of the train, S is the maximum cross-sectional area of the train(11.2m^2).

In the Fig.13 and Fig.14, the dimensionless aerodynamic forces of the pantograph are shown, it can be seen that the coefficient of aerodynamic force of the pantograph is consistent with the different running speed in the tunnel. However, due to different running speed, the position of the pantograph intersecting with the expansion wave is different, which leads to the different decrease position of the aerodynamic force of the pantograph. In the middle and at the exit of the tunnel, there are difference about the coefficient of the aerodynamic lift of the pantograph.

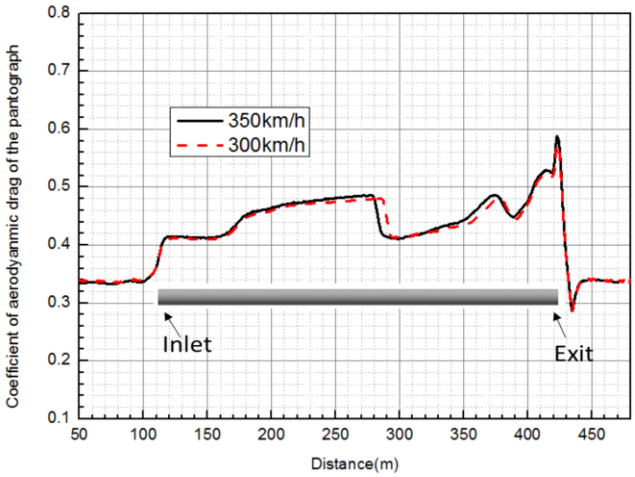

Fig.13 The dimensionless aerodynamic drag variation vs. distance

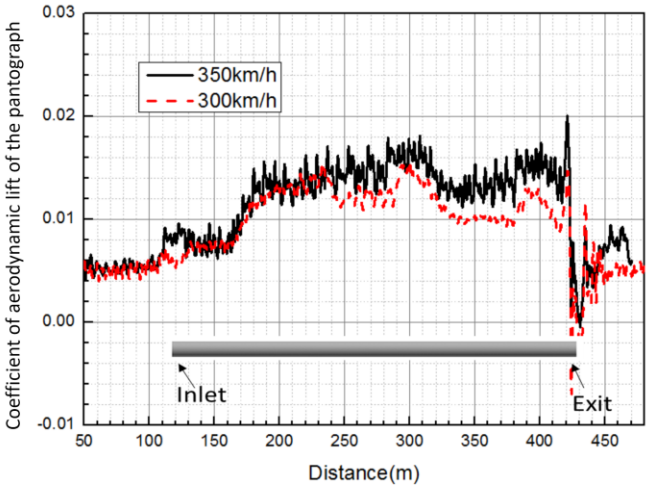

Fig.14 The dimensionless aerodynamic lift variation vs. distance

CONCLUSION

In this paper, with IDDES method combined overset grid technique, the variation of the aerodynamic force of the pantograph is studied when the high-speed train passes through the tunnel. The results can be presented as follows:

When the train is running with high speed, a series of vortices are formed at the wake of the pantograph, which make the aerodynamic force of the pantograph exhibit obvious unsteady characteristics.

When the high-speed train passes through the tunnel, the aerodynamic force of the pantograph changes strongly. When the pantograph is entering the tunnel, the pantograph is subject to a dramatic increase in aerodynamic forces. In the middle of the tunnel, due to the effect of the expansion wave, the aerodynamic force of the pantograph decreases dramatically. At the exit of the tunnel, the pantograph is subjected to the most severe aerodynamic force changes.

When the high-speed train passes through the tunnel at different speed, the aerodynamic force of the pantograph is consistent, however, due to the difference of the speed, the position of the intersection of the pantograph and the expansion wave is different, which leads to the different decline position of the pantograph aerodynamic force in the tunnel.

ACKNOWLEDGMENTS

This paper is funded by the National Key Research and Development program under 2016YFB1200506.

REFERENCES

1. Mei, G.M. The dynamics study of pantograph/catenary system [D].Southwest Jiaotong University. 2010.
2. Li, D.Y. The experimental research of pantograph's vibrational characteristic [D]. Southwest Jiaotong University. 2012.
3. Tian, H.Q. Train aerodynamics [M]. China railway publishing house. 2007.
4. Mei, Y.G, Zhou, C.H, Xu, J.L. Aerodynamics of high speed railway tunnel [M]. Science press. 2009.
5. Wang, J.Y, Wan, X.Y, W, J. Influence of tunnel lengths upon air pressure fluctuation in high speed railway tunnels [J]. Modern tunneling technology. 2008, 45(6)
6. J. Pombo. Influence of the aerodynamic forces on the pantograph-catenary system for high-speed trains [J]. Vehicle system dynamics. 2009, 47(11).
7. M. Bocciolone, F. Resta, D. Rocchi, A. Tosi&A. Collina. Pantograph aerodynamic effects on the pantograph–catenary interaction [J]. Vehicle system dynamics. 2006, 44(1).
8. Li. R.P, Zhou. N, Zhang, W.H. Calculation and analysis of pantograph aerodynamic uplift force [J]. Journal of the china railway society. 2012-08.
9. Guo. D.L, Yao. S.B. the study of the unsteady aerodynamic characteristic of the pantograph of high-speed train [J]. Journal of the china railway society. 2012-11.
10. Yao. Y, Guo. D.L. The unsteady aerodynamic characteristic of high speed pantograph [J]. Computer aided engineering. 2012-10.
11. Railway applications. Aerodynamics. Requirements and test procedures for aerodynamics in tunnels. En 14067-5 2006.
12. Star-ccm+ Documentation v9.04